COLLECTIVE MOTION

The behavioral mechanisms governing collective motion in swarming locusts

Sercan Sayin[1,2,3]*, Einat Couzin-Fuchs[1,2,3], Inga Petelski[1,2,3], Yannick Günzel[1,2,3], Mohammad Salahshour[1,2,3], Chi-Yu Lee[1,3], Jacob M. Graving[1,2,3,4], Liang Li[1,2,3], Oliver Deussen[1,5], Gregory A. Sword[6], Iain D. Couzin[1,2,3]*

Collective motion, which is ubiquitous in nature, has traditionally been explained by "self-propelled particle" models from theoretical physics. Here we show, through field, lab, and virtual reality experimentation, that classical models of collective behavior cannot account for how collective motion emerges in marching desert locusts, whose swarms affect the livelihood of millions. In contrast to assumptions made by these models, locusts do not explicitly align with neighbors. While individuals respond to moving-dot stimuli through the optomotor response, this innate behavior does not mediate social response to neighbors. Instead, locust marching behavior, across scales, can be explained by a minimal cognitive framework, which incorporates individuals' neural representation of bearings to neighbors and internal consensus dynamics for making directional choices. Our findings challenge long-held beliefs about how order can emerge from disorder in animal collectives.

Theoretical models from physics, such as the highly influential Vicsek model (*1*), describe how simple local interactions, where individuals align their movement with nearby individuals, can generate large-scale, coordinated (meaning aligned or ordered) motion in groups. This model makes the prediction that groups should exhibit a spontaneous transition between two collective states—from a disordered state (akin to a gas) to an ordered state (akin to a driven fluid)—as density increases. This concept has implications for understanding collective behavior across biological systems, from cellular aggregates to human crowds.

The results of empirical studies, including experiments with juvenile desert locusts (*Schistocerca gregaria*), have lent support to this theory. Locust swarms, which can cover vast areas and greatly impact food security (*2*), serve as a prominent example of collective motion. Laboratory findings have suggested that increasing locust density in a ring-shaped arena leads to a shift from disordered to ordered motion, appearing to validate the predicted density-dependent phase transition (*3*). Thus, despite inherent errors in individual alignment, a sufficient density of individuals is argued to enable an averaging out of noise and the emergence of coherent group movement. In general, comparison of model predictions and empirically observed collective motion has provided evidence supporting these "classical" models of collective behavior (*3*–*8*).

There exists an inherent problem with this approach, however. Given that density and order are positively correlated, it is challenging to establish cause and effect. This raises the question of whether alignment results from the averaging out of uncorrelated errors at high densities, as classical theory suggests, or whether the coherence of motion itself triggers alignment, independent of density. That is, is it the density (corresponding to the "amount" of information) or the order (the "quality" of information) that is predominantly important or rather how the two interact? Furthermore, do individuals explicitly align their direction of travel with near neighbors, as is assumed in these classic models? Addressing these questions is crucial not only for understanding the fundamentals of biological collective motion but also for gaining insights into the formation and maintenance of locust swarms, which affect human well-being (*2*).

Using a combination of field experiments with naturally occurring locust swarms and analysis of how visual interactions are mediated using immersive virtual reality (VR) (*9*, *10*), we reveal that classical models of collective behavior [such as the Vicsek model (*1*) and Couzin model (*11*–*13*)] cannot account for collective motion exhibited by locusts and that the mechanism proposed for the emergence of their collective motion needs to be corrected. We demonstrate that locusts do not explicitly align with neighbors and that their behavior is consistent with a minimal cognitive model of spatiotemporal decision-making. We argue for an approach to the study of collective behavior that moves from descriptive to generative models, with the latter taking into account that organisms are not self-propelled particles but rather probabilistic decision-making entities that base their decisions explicitly on the representation and integration of sensory information.

Field experiments

The largest East African outbreak of the desert locust in recent years began in late 2019. In February 2020, we conducted experiments on large "marching bands" of flightless juvenile locusts in the Samburu and Isiolo counties of Kenya to establish the predominant sensory modalities used in coordinating motion. Swarms of locust nymphs were encountered at a large number of locations, ranging from first to sixth instar (juvenile) stages (Fig. 1, A and B). In 56 cases where we recorded marching band directions, a prominence along the north/northeast axis was noted (Fig. 1B and table S1). Consistent with previous studies (*14*), marching direction did not clearly relate to immediate weather conditions, elevation, or sun position (fig. S1).

To assess the role of different modalities used by focal locusts in maintaining coordinated group movement, we independently manipulated olfaction (by clipping antennae), polarized vision (by painting ocelli and the dorsal rim area of the compound eyes), and vision (by painting ocelli and the entirety of the compound eyes). Control insects were similarly handled but left with their senses intact. All insects were painted with an identifiable color marking on their pronotum before being returned to an undisturbed section of the marching band.

Reintroduced control locusts, anosmic locusts, and locusts deprived of polarized vision exhibited a strong, and rapid, tendency to march with, and in the direction of, conspecifics in the band (Fig. 1C, i, ii, and iii, respectively). Completely blinded insects, by contrast, moved in random directions with respect to the band direction (Fig. 1C, iv, and E). Although these blinded individuals remained mobile—likely owing to tactile cues that increase movement probability to avoid cannibalistic interactions (*15*–*17*)—in many cases, contact alone did not provide directional guidance, even in densely packed, highly directional swarms. Thus, we conclude that vision is both necessary and sufficient for individuals to coordinate motion with neighbors.

VR experiments

As noted above, there has been a confound in previous approaches to establish the mechanism by which locusts regulate their behavior in swarms because of the inherent (theoretical) positive correlation between density and order. To decouple these two factors, we enabled

[1]Centre for the Advanced Study of Collective Behaviour, University of Konstanz, Konstanz, Germany. [2]Department of Collective Behavior, Max Planck Institute of Animal Behavior, Konstanz, Germany. [3]Department of Biology, University of Konstanz, Konstanz, Germany. [4]Advanced Research Technology Unit, Max Planck Institute of Animal Behavior, Konstanz, Germany. [5]Department of Computer and Information Science, University of Konstanz, Konstanz, Germany. [6]Department of Entomology, Texas A&M University, College Station, TX, USA.
*Corresponding author. Email: icouzin@ab.mpg.de (I.D.C.); sercan.sayin@uni-konstanz.de (S.S.)

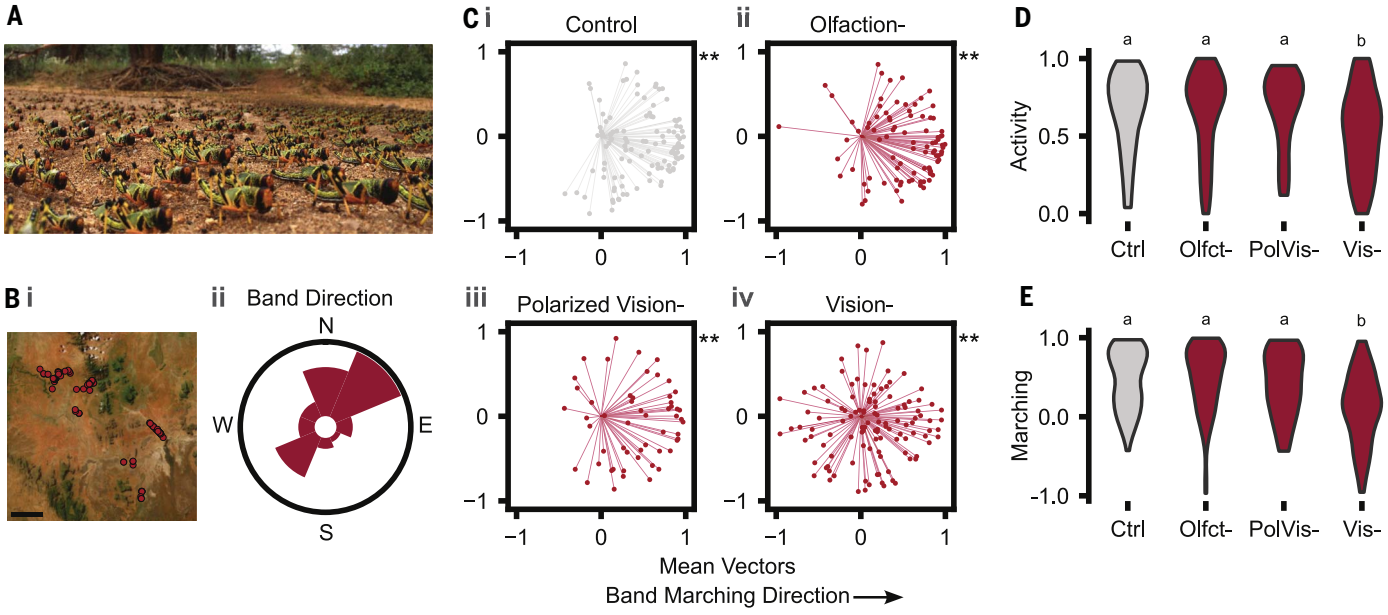

Fig. 1. Sensory deprivation experiments in the field. (**A**) A marching band of *S. gregaria* photographed in Kenya in 2020. (**B**) (i) Locust bands in a total of 112 locales between 27 February and 12 March of 2020 in the Samburu and Isiolo districts of Kenya. Scale bar: 15 km. (ii) Observed marching band directions. n = 56 bands. Histogram counts: min = 2, max = 23. (**C**) Single tagged locusts were reintroduced to a marching band after antennectomy (Olfaction−, n = 89) or visual occlusion (Polarized Vision−: dorsal eyes and ocelli, n = 54; Vision−: complete eyes and ocelli, n = 114). Control n = 110. Locust movements were reported as mean vectors. Statistical annotations on each upper right corner stand for the results of Rayleigh test for nonuniformity. (**D** and **E**) Mean binarized Euclidean distance (Activity) and mean vector magnitude in congruence with marching band (Marching) by control and treated animals. Olfct, olfaction; PolVis, polarized vision; Vis, vision. See table S2 for statistical summaries.

real locusts to interact with virtual conspecifics. Notably, our system was fully panoramic, allowing untethered, freely moving locusts to interact with visual stimuli from fully volumetric three-dimensional ("holographic") marching conspecifics with no constraints resulting from boundaries (Fig. 2, A and B).

In order to conduct a full parametric scan of density-order space, we considered independent combinations of density, from 1 to 64 locusts per m^2, and order (from 0, equivalent to randomly moving individuals, to 1, where virtual conspecifics are in perfect alignment with one another) (Fig. 2, C and D). We note that our upper and lower insect densities exceed the range tested (2 to 62 moving locusts per m^2) by Buhl *et al.* (*3*).

Locusts' alignment with the virtual swarm was found to strongly depend on the order parameter, that is, the "quality" of information presented, with no significant dependency on density (Fig. 2, E to G, and fig. S4A). With higher order, focal locusts marched longer distances in more-directed trajectories (max: 46.1 m; figs. S3 and S4A, i and ii). We note that the cumulative distances covered by focal insects were comparable between different order and density conditions (fig. S4A, iii). Clearly, if no directional cues are present, locusts have no social context on which to base their movements, but we find that even with very sparse but high-quality (i.e., ordered) information, they exhibit a strong tendency to align with the motion of others. Notably, while these results are apparently in contradiction to the data of Buhl *et al.* (*3*), a reevaluation of their data, taking into account statistical effects associated with different group sizes, reveals that collective alignment (order) is also independent of locust density in these experiments (fig. S6).

Behavioral response to optical flow

It has long been considered that coherent motion in animal groups may be mediated by the optomotor response. If animals, such as insects or fish, are presented with coherently moving dots or stripes, they will tend to move in the direction of the resulting optical flow stimulus. Being an innate and robust behavior, optical flow is often intuitively considered an important if not essential mechanistic basis of collective motion in large mobile groups [see (*18*, *19*) for fish and (*20*, *21*) for locusts]. Yet, direct evidence in support of this hypothesis is lacking. Recently, Bleichman *et al.* (*20*) presented coherent moving dots on either side of a rigidly tethered locust and demonstrated that the motion could alter the probability of the locust moving. However, the focal locusts in this study were constrained to only be fully aligned with the stimuli and could not alter their direction in response to stimuli.

We assessed whether locusts are sensitive to optical flow under conditions where they could freely move with respect to the presented cue. In evaluating this, we took advantage of the fact that locusts exhibit extreme phenotypic plasticity, including in social behavior. If reared in isolation, locusts are sedentary insects that avoid conspecifics, a phenotype that is referred to as "solitarious" (*22*–*24*). It is only when they are reared together that they become "gregarious" and exhibit increased activity and attraction to other locusts (*22*–*24*). Should optomotor response to optical flow cues underlie the alignment among individuals in swarms, we may expect that gregarious locusts would be more responsive to such cues than are solitarious insects.

We find that this is not the case. Both solitarious and gregarious locusts exhibit a similar propensity to turn in the direction of the wide-field moving-dot stimulus, with solitarious insects exhibiting a slightly stronger response (Fig. 3A). However, when placed in a coherently moving virtual swarm, solitarious insects do not align their direction of travel with the virtual conspecifics (Fig. 3B), whereas gregarious individuals strongly do so (Figs. 2 and 3B). These results are inconsistent with the view that the optomotor response is involved in regulating social interactions in marching locusts.

The role of "pull" in swarms

Another aspect that classical collective movement models and the optical flow hypothesis

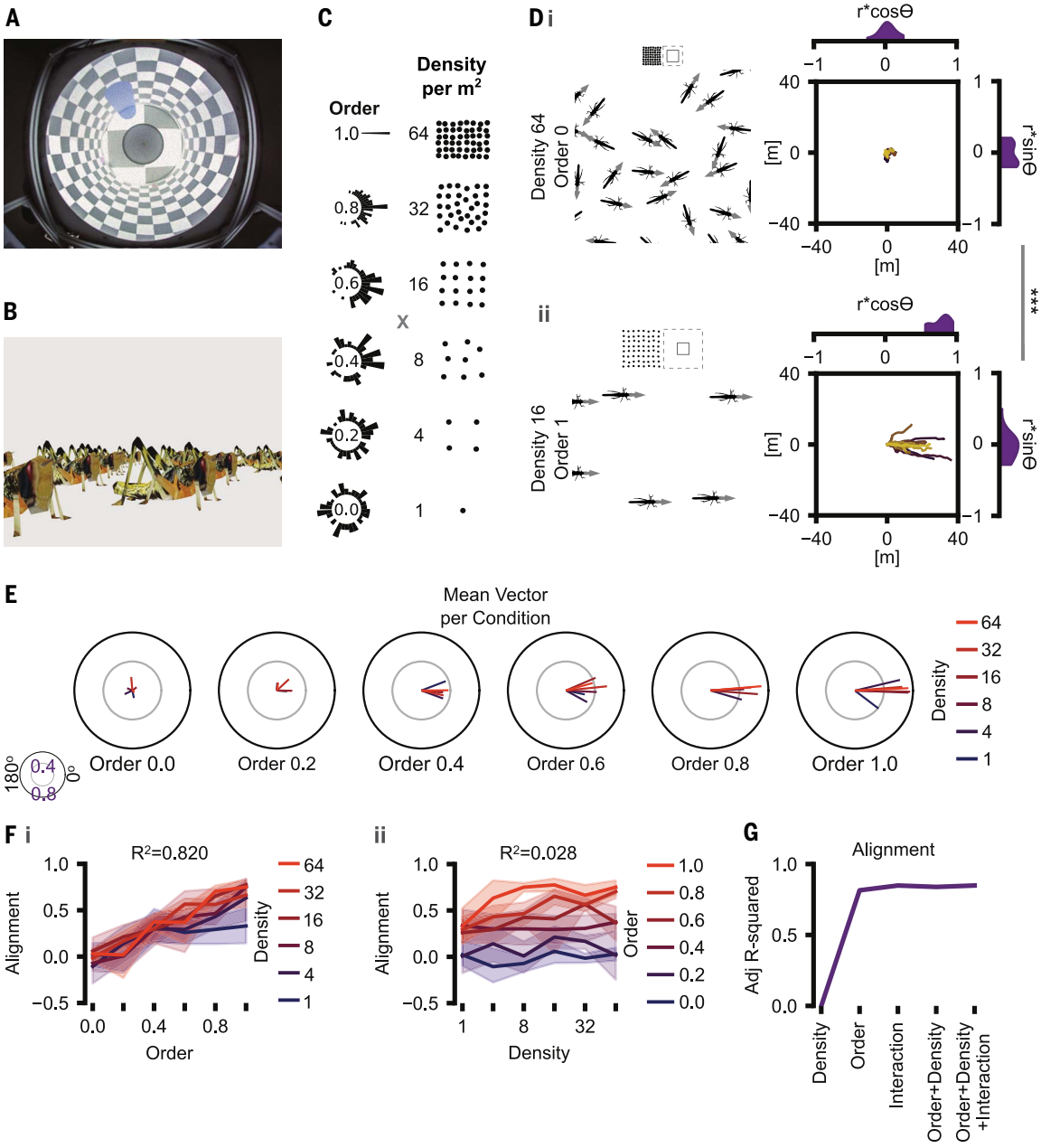

Fig. 2. Reconstructing marching in an immersive virtual reality. (**A**) Top-down view of the virtual reality system. A motion compensation system stabilizes an untethered fifth instar desert locust in position, and from this perspective, a panoramic virtual world is projected in 100-Hz high refresh rate. (**B**) Virtual marching band. The virtual reality engine draws animated juvenile desert locust visual stimuli with real-world kinematics data (fig. S2) and constant velocity. Throughout an experiment, periodic boundaries set for virtual band guarantee that the experimental focal juvenile locust is located at the virtual band's center. (**C**) Experimental design. Virtual bands were generated to vary by two parameters, order and marching band density per square meter. For a given order value, von Mises distributions constituted a marching band's coherence de novo. Focal locusts were tested once for one condition per 20 min. Completed trials equaled 421 once outliers were removed. See the methods section of the supplementary materials for details of the experimental design and the analysis pipeline. (**D**) Exemplary order and density combinations. Schematics depict virtual locust positions and directions at a given time. Above each schematic, periodic boundaries and zoomed areas are drawn with dashed and solid lines, respectively. All bands consist of 64 virtual locusts. Individual trajectories per condition are shown on the right. n = 13 for both groups. Mean vector (**r**) projections onto axes congruent with (**r***cosθ) and perpendicular to (**r***sinθ) marching band directions were used for multivariate analyses. To see all trajectories, refer to fig. S3. (**E**) Means per each condition of 64 order and density combinations. (**F**) Alignment (calculated as **r***cosθ) versus order (i) and density (ii) as primary parameters for reporting. Color codes designate secondary parameter. Coefficient of determination (R^2) scores showcase explanatory power of respective primary parameters alone. See comparison of directedness, marching, and Euclidean distances with respect to either density or order "alone" in fig. S4. See fig. S5 for clustering of all data groups. (**G**) Adjusted R^2 from ordinary least squares regression models on alignment group means for different explanatory variables used. See table S2 for statistical summaries.

do not consider is the frame of reference of focal individuals with respect to the direction of collective movement (*1*, *21*). Addressing this, later models, again relying on theoretical physics, speculated whether collective motion can be generated by collisions and escape and pursuit mechanisms (*25*, *26*). We devised a scenario to test how visual stimuli from receding swarms of virtual insects affect the behavior of focal locusts. In this condition, highly ordered marching bands at a 5-cm offset from focal positions were generated (Fig. 4A). Virtual locusts presented as moving away were sufficient to recapitulate focal locust alignment behavior with comparable distances covered as in the full virtual marching band conditions (Fig. 4B, compare with Fig. 2D, ii). Furthermore, our analysis of neighbor positions for locusts

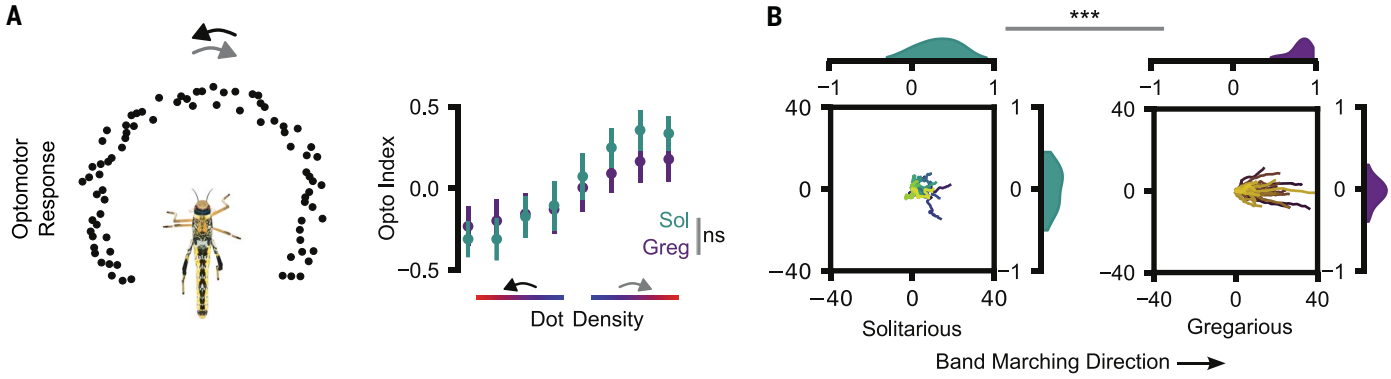

Fig. 3. Optical flow does not drive marching. (**A**) (Left) The moving-dot paradigm schematic used in the study. (Right) Optomotor responses of solitarious (Sol) and gregarious (Greg) desert locusts to moving-dot stimuli of different densities, color coded blue to red for low to high density. All stimuli have 100% coherence, meaning that the moving dots in an experiment move either counterclockwise or clockwise. The optomotor response, or opto-index, is a preference index calculated as the difference between summed absolute counterclockwise and clockwise velocities, then dividing that difference by the sum of these velocities for a given trial. n = 32 locusts tested. Number of dots in the density paradigm was 64, 256, 1024, and 4096. (**B**) Trajectories for solitarious locusts (n = 34) and gregarious control locusts (n = 32) within a virtual gregarious marching band (order: 1; density: 16). See table S2 for statistical summaries.

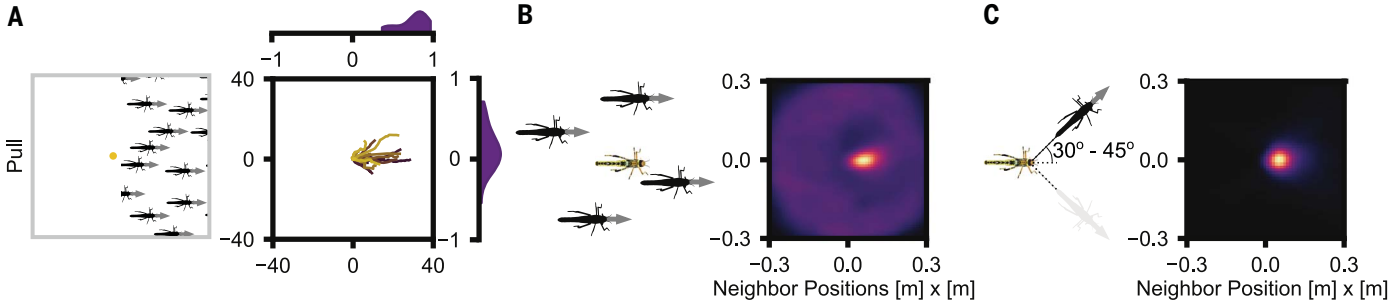

Fig. 4. Attraction to conspecifics for locust virtual bands. (**A**) Pull experimental design. A focal locust is positioned immediately behind a highly ordered marching band. n = 21. Periodic boundaries ensured constant distance between focal locust and marching band edge. See fig. S7 for "Push" condition. Figure S9 explores roles of order and distance in pull conditions. (**B**) Density map for egocentric neighbor positions in a highly ordered marching as in Fig. 2D. Focal heading is along +x axis. Focal n = 22. See fig. S10 for neighbor-follow duration. (**C**) Density map for neighbor positions in single virtual locust assay. A single virtual locust, with constant velocity, was positioned in front of focal locust, at 30° to 45° offset. A single trial lasted as long as the distance between follower focal locust and virtual target was maintained within a threshold distance (50 cm). Focal heading is along +x axis. Focal n = 12. Normalized densities are displayed with a color gradient from dark purple for the minimum to bright yellow for the maximum. See fig. S10 for neighbor-follow durations.

surrounded by conspecifics in a full marching band and in experiments when only one receding virtual locust was present showed that focal individuals closely follow neighbors (Fig. 4, C and D). As a validation of our VR experiments, quantification of locust interactions in an arena experiment with 2000 locusts revealed a similar proximal pursuit mechanism in real-world interactions as well (fig. S11). These results show that moving-away conspecifics play a strong "pulling" role in the regulation of marching behavior, consistent with a mechanism involving pursuit.

A vectorial representation of conspecifics

Our above findings show that locusts may not base decisions on simple fixed "rules." An alternative framework considers the generative process by which decisions are made; for example, Sridhar *et al.* (*10*) developed a model of spatial decision-making based on neural principles. Consistent with neurobiological studies of insects (*27*, *28*) and vertebrates (*29*), neighbors are considered to induce neural activity bumps on a "ring attractor" network, with their position on the ring reflecting their bearing with respect to the focal animal. Given that neural activity encodes both directional information (bearings) and the "strength" of influence (encoded by the magnitude of neural activity), this is a "vectorial representation" of conspecifics. Ongoing internal dynamics on the ring attractor network, defined predominantly by local excitation and long-range and/or global inhibition, facilitate the integration of these sensory inputs, generating a self-organized bump of activity on the ring (a collective neural consensus mechanism) that represents the animal's subsequent directional preference [for details, see (*10*, *30*, *31*)].

This type of cognitive model, which we refer to as the vectorial hypothesis, makes directly testable predictions with respect to behavior, and these predictions are in stark contrast to those of the optical flow hypothesis. For example, if presented with two conspecifics moving in the same direction and speed at a fixed lateral distance (L) (Fig. 5A), our model predicts that a follower should occupy, on average, a position directly between them, up to a critical distance above which there should

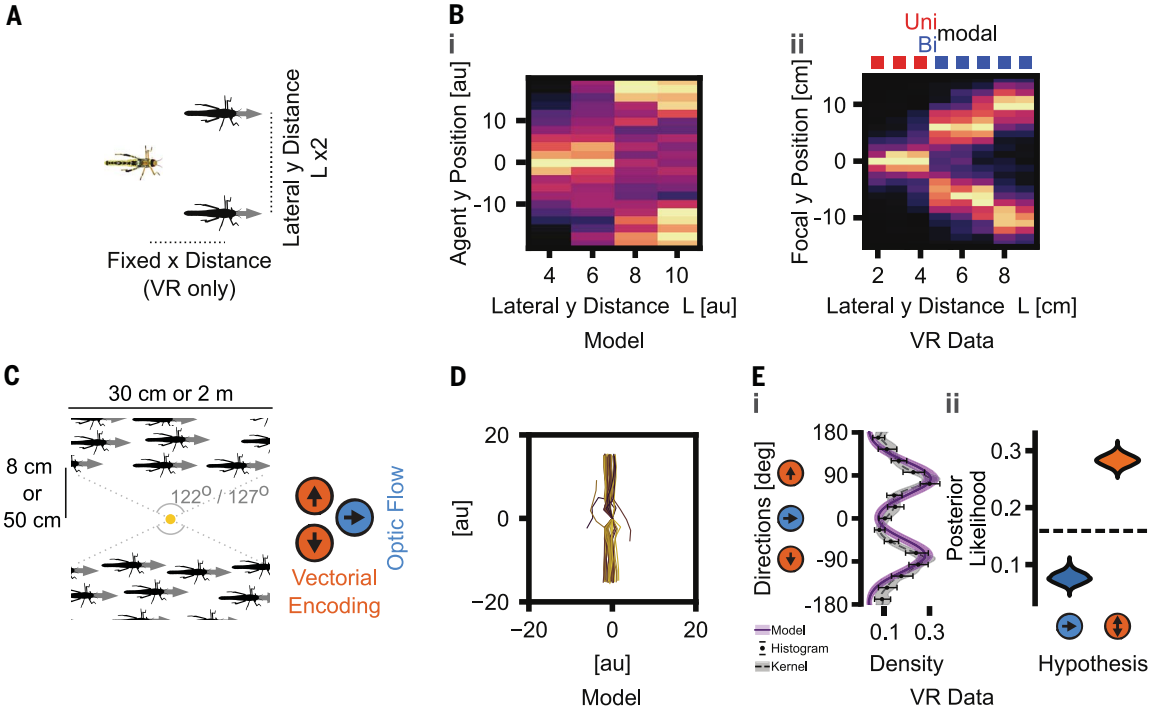

Fig. 5. Vector computations can explain individuals' response to conspecifics. (**A**) Schematic of the two conspecific "targets" scenario used in our simulation model and VR experiments. Lateral distance (along *y* axis) between two targets was set to constant at 2× *L*. In all VR trials, horizontal distance (along *x* axis) between focal locust and two targets was fixed. (**B**) (i) Model agent *y* positions when a focal agent is presented with two moving targets. au, arbitrary units. See fig. S12 for two-dimensional position histograms. *n* = 200 for all conditions. (ii) Instances in VR where focal locust followed targets depicted as a heatmap as in focal individual's *y* position versus lateral distance *L*. Dip test of unimodality is used to assess *y* position distribution (red: $P > 0.05$; blue: $P < 0.05$). Focal locust *n* = 11. Histogram range is displayed with a color gradient from dark purple for the minimum to bright yellow for the maximum. (**C**) Experimental design to evaluate the possible roles of optical flow versus vectorial representation in coordinating marching for VR experiments. At a given fixed lateral distance (8 or 50 cm) to the focal locust, two highly ordered bands move in same direction. Each virtual locust has a 100-ms life span, to preserve optical flow and positional cues but to prevent the focal locust from persistently "locking onto" a single target. (**D**) Trajectories of simulated agents. Similar to (C), an agent is placed in between two sets of targets moving in the same direction. The initial lateral distance of the agent to targets was 20 au. Trajectories plotted for the first 20 au covered by each agent. *n* = 100. (**E**) Hierarchical Bayesian model used to infer predominant movement directions in VR scenarios tested as in (C). (i) The posterior model density compared with nonparametric bootstrapped histogram density and kernel density estimates (see materials and methods for details). Lines and points show the median of the posterior or bootstrap distribution, whereas the bars and bands show the 95% interval (2.5 to 97.5%; *n* = 4000 samples per density type). (ii) Distributions of posterior likelihood scores for hypothesis testing. *n* = 4000 samples per hypothesis. Dashed line represents a random walk hypothesis as a uniform likelihood. Figure S14 offers focal locust trajectories for both conditions tested in (C). Tested locusts *n* = 50. See table S2 for statistical summaries.

exist a dynamical bifurcation in the neural dynamics, resulting in a decision to choose to follow one or the other. That is, the brain should suddenly transition between an "averaging" and a "winner takes all" dynamic (*10*). The optomotor (optical flow) hypothesis, by contrast, predicts that a focal locust should align with conspecifics irrespective of their lateral distance. In both models, there exists a further, maximal distance at which interactions become impossible owing to insufficient sensory information.

Presenting a pair of marching virtual conspecifics with different lateral distances, we see, as predicted by the vectorial hypothesis (Fig. 5B, i), a clear bifurcation in the relative position adopted by the real locust (Fig. 5B, ii). We note that in conventional laboratory experiments with real interacting insects, it is not possible to conduct such a test of the underlying cognitive mechanism, thus highlighting an advantage of the VR approach for establishing the nature of visual social interactions.

A further, complementary experiment to test the mechanistic basis of social interactions is how a focal locust will behave if positioned directly between two coherently marching swarms. In classic models of collective behavior that include attraction, the symmetry of attractive "forces" in one direction and the other would result in them tending to cancel out, and an explicit alignment term, if present, would dominate, resulting in alignment with directional cues (see supplementary text in the supplementary materials). Similarly, the optical flow hypothesis would predict motion in alignment with swarm direction. The cognitive model, by contrast, which only considers attraction but captures the competition between conflicting directional information (owing to the presence of long-range inhibition), predicts that in this scenario, locusts should move in a direction perpendicular to the swarm motion. To evaluate these hypotheses, locusts were placed at a fixed equal distance (either 8 or 50 cm) in between two parallel virtual marching bands, both moving in the same direction (Fig. 5C). Here, optical flow is parallel to marching direction (+*x* axis, as indicated by the blue circle), while vectors representing conspecifics are (approximately) perpendicular (±*y* axis, as indicated by the orange circles) to the collective movement. For model agents (Fig. 5D) and focal locusts (Fig. 5E and fig. S14), movement direction was predominantly directly toward one marching band or the other and not in congruence with optical flow (or with classic self-propelled particle models; see supplementary text).

Our results suggest that locust marching behavior is mediated by a vectorial encoding strategy and not a strategy that uses explicit alignment. To establish whether individuals utilizing this same mechanism can account for the emergence of long-range coordinated motion in locusts, we also considered the scenario of conspecific representation as (competing) bumps on a neural ring attractor network (see supplementary materials for details), revealing

that it can account for the emergence of highly ordered collective motion (fig. S15).

Conclusions

Our work suggests that, contrary to previous assertions, classical models of collective motion fail to account for the mechanism by which coherent motion is established and maintained in desert locust swarms. For example, we found no evidence that locusts explicitly align with one another nor that they use the optomotor response to mediate social interactions. Furthermore, both our data and a critical revaluation of those of Buhl *et al.* (*3*) find no evidence for a density-dependent transition from disorder to ordered swarm motion, further questioning the dominant paradigm used to study animal collectives more broadly. By contrast, we find that individual and collective locust behavior is consistent with a minimal cognitive model (a ring attractor network) in which individuals (targets) are represented as competing neural bumps. This suggests that wide-field optical flow cues (such as those used for self-motion estimation and/or wide-field landscape information) are separate from those cues used in neighbor tracking. Circuits responsible for pursuing neighbors are yet to be described for locusts. Beyond a simple detection of objects against a moving background, vectorial representation and wide-field motion necessitate competition under certain scenarios, and how global information is suppressed is yet to be explored. Revealing these circuits will enable the identification of afferent and modulatory inputs, which will be instrumental to infer causality regarding the forces that govern pursuit and collective motion. Furthermore, given the clear discrepancy between gregarious and solitarious behavior in locusts, we suggest future exploration of differential modulation or developmental regulation of visual attraction and decision-making networks. Our work argues for a refreshed perspective in the study of collective animal behavior that moves beyond the "self-propelled particle" paradigm and considers explicitly the sensory and cognitive mechanisms by which interactions are mediated.

REFERENCES AND NOTES

1. T. Vicsek, A. Czirók, E. Ben-Jacob, I. Cohen, O. Shochet, *Phys. Rev. Lett.* **75**, 1226–1229 (1995).
2. A. Steedman, *Locust Handbook* (Natural Resources Institute, 1990).
3. C. Buhl *et al.*, *Science* **312**, 1402–1406 (2006).
4. J. Buhl, G. A. Sword, S. J. Simpson, *Interface Focus* **2**, 757–763 (2012).
5. D. J. T. Sumpter, R. P. Mann, A. Perna, *Interface Focus* **2**, 764–773 (2012).
6. R. Lukeman, Y.-X. Li, L. Edelstein-Keshet, *Proc. Natl. Acad. Sci. U.S.A.* **107**, 12576–12580 (2010).
7. R. P. Mann *et al.*, *PLOS Comput. Biol.* **9**, e1002961 (2013).
8. Ch. Becco, N. Vandewalle, J. Delcourt, P. Poncin, *Physica A* **367**, 487–493 (2006).
9. J. R. Stowers *et al.*, *Nat. Methods* **14**, 995–1002 (2017).
10. V. H. Sridhar *et al.*, *Proc. Natl. Acad. Sci. U.S.A.* **118**, e2102157118 (2021).
11. I. D. Couzin, J. Krause, R. James, G. D. Ruxton, N. R. Franks, *J. Theor. Biol.* **218**, 1–11 (2002).
12. I. D. Couzin, J. Krause, N. R. Franks, S. A. Levin, *Nature* **433**, 513–516 (2005).
13. I. D. Couzin *et al.*, *Science* **334**, 1578–1580 (2011).
14. P. E. Ellis, C. Ashall, *Field Studies on Diurnal Behaviour, Movement and Aggregation in the Desert Locust (Schistocerca gregaria Forskål)* (Anti-Locust Research Centre, 1957).
15. S. Bazazi *et al.*, *Curr. Biol.* **18**, 735–739 (2008).
16. S. J. Simpson, G. A. Sword, P. D. Lorch, I. D. Couzin, *Proc. Natl. Acad. Sci. U.S.A.* **103**, 4152–4156 (2006).
17. H. Chang *et al.*, *Science* **380**, 537–543 (2023).
18. R. Harpaz *et al.*, *Sci. Adv.* **7**, eabi7460 (2021).
19. E. Shaw, B. D. Sachs, *J. Comp. Physiol. Psychol.* **63**, 385–388 (1967).
20. I. Bleichman, P. Yadav, A. Ayali, *Proc. Biol. Sci.* **290**, 20221862 (2023).
21. D. L. Krongauz, A. Ayali, G. A. Kaminka, *PLOS Comput. Biol.* **20**, e1011796 (2024).
22. M. P. Pener, S. J. Simpson, *Adv. Insect Physiol.* **36**, 1–272 (2009).
23. S. M. Rogers *et al.*, *J. Insect Physiol.* **65**, 9–26 (2014).
24. H.-J. Pflüger, P. Bräunig, *J. Comp. Physiol. A* **207**, 321–326 (2021).
25. P. Romanczuk, I. D. Couzin, L. Schimansky-Geier, *Phys. Rev. Lett.* **102**, 010602 (2009).
26. D. Grossman, I. S. Aranson, E. Ben Jacob, *New J. Phys.* **10**, 023036 (2008).
27. J. D. Seelig, V. Jayaraman, *Nature* **521**, 186–191 (2015).
28. C. Lyu, L. F. Abbott, G. Maimon, *Nature* **601**, 92–97 (2022).
29. A. Sarel, A. Finkelstein, L. Las, N. Ulanovsky, *Science* **355**, 176–180 (2017).
30. L. Oscar, L. Li, D. Gorbonos, I. D. Couzin, N. S. Gov, *Phys. Biol.* **20**, 045002 (2023).
31. D. Gorbonos, N. S. Gov, I. D. Couzin, *PRX Life* **2**, 013008 (2024).
32. S. Sayin *et al.*, The Behavioral Mechanisms Governing Collective Motion in Swarming Locusts [Data set], Zenodo (2025); https://doi.org/10.5281/zenodo.14353283.
33. S. Sayin *et al.*, The Behavioral Mechanisms Governing Collective Motion in Swarming Locusts (Subrepository3), Zenodo (2025); https://doi.org/10.5281/zenodo.14355590.

ACKNOWLEDGMENTS

The authors thank student assistants M. C. Karakurt, J. Klein, and Z. Sener for VR data collection; E. Mamonova, H. Kübler, and N. Schwarz for tracking field data; L. Schröder and N. Schwarz for trackball data collection; F. Oberhauser for being an invaluable team member in Kenya; M. Mahmoud for contributing to VR development in its early phases; A. Bahl and K. Slangewal for implementing real-time orientation tracking in VR; and D. S. Calovi for experimental design discussions. J.M.G. thanks J. Bak-Coleman for help with model debugging and M. L. Smith for the use of his GPU. J.M.G. acknowledges support from NVIDIA Corporation's Academic Hardware Grant Program. We thank C. Buhl and K. Yates for providing Buhl *et al.* (*3*) data. We also thank C. Buhl for feedback on the manuscript. We acknowledge the use of ChatGPT, a language model developed by OpenAI, for minor suggestions with respect to the text, equations, software, and figures. **Funding:** Deutsche Forschungsgemeinschaft (DFG, German Research Foundation) under Germany's Excellence Strategy–EXC 2117-422037984. To E.C.-F.: DFG GZ: CO 1758/5-1. To I.D.C.: the Max Planck Society, the European Union's Horizon 2020 Research and Innovation Programme under Marie Skłodowska-Curie Grant 860949, the DFG Gottfried Wilhelm Leibniz Prize 2022 584/22, the Struktur- und Innovationsfonds für die Forschung of the State of Baden-Württemberg, the PathFinder European Innovation Council Work Programme 101098722, and the Office of Naval Research Grant N0001419-1-2556: To G.A.S.: NSF Biology Integration Institute Program Grant DBI-2021795. **Author contributions:** Conceptualization: S.S., E.C.-F., G.A.S., I.D.C.; Formal analysis: S.S., M.S., C.-Y.L., J.M.G., L.L., I.D.C.; Funding acquisition: O.D., E.C.-F., I.D.C.; Investigation: S.S., E.C.-F., I.P., C.-Y.L., I.D.C.; Methodology: S.S., E.C.-F., J.M.G., I.D.C.; Project administration: E.C.-F., I.D.C.; Resources: Y.G., J.M.G., L.L., I.D.C.; Supervision: E.C.-F., I.D.C.; Validation: S.S., Y.G., J.M.G., I.D.C.; Visualization: S.S., J.M.G.; Writing – original draft: S.S., I.D.C.; Writing – review & editing: S.S., E.C.-F., Y.G., M.S., C.-Y.L., J.M.G., L.L., O.D., G.A.S., E.C.-F., I.D.C. **Competing interests:** The authors declare that they have no competing interests. **Data and materials availability:** The source data and material (*32*) and the analysis scripts (*33*) are available in Zenodo.

SUPPLEMENTARY MATERIALS

science.org/doi/10.1126/science.adq7832
Materials and Methods
Supplementary Text
Figs. S1 to S15
Tables S1 and S2
References (*34*–*48*)
MDAR Reproducibility Checklist

Submitted 5 June 2024; accepted 20 December 2024
10.1126/science.adq7832